JOURNAL OF
GENERAL VIROLOGY

RESEARCH ARTICLE
Scherbatskoy *et al.*, *Journal of General Virology*
DOI 10.1099/jgv.0.001421

MICROBIOLOGY SOCIETY

Characterization of a novel picornavirus isolated from moribund aquacultured clownfish

Elizabeth C. Scherbatskoy[1], Kuttichantran Subramaniam[1], Lowia Al-Hussinee[1], Kamonchai Imnoi[1], Patrick M. Thompson[1]†, Vsevolod L. Popov[2], Terry Fei Fan Ng[3], Karen L. Kelley[4], Rodolfo Alvarado[4], Jeffrey C. Wolf[5], Deborah B. Pouder[6], Roy P.E. Yanong[6] and Thomas B. Waltzek[1,*]

Abstract

Over the last decade, a number of USA aquaculture facilities have experienced periodic mortality events of unknown aetiology in their clownfish (*Amphiprion ocellaris*). Clinical signs of affected individuals included lethargy, altered body coloration, reduced body condition, tachypnea, and abnormal positioning in the water column. Samples from outbreaks were processed for routine parasitological, bacteriological, and virological diagnostic testing, but no consistent parasitic or bacterial infections were observed. Histopathological evaluation revealed individual cell necrosis and mononuclear cell inflammation in the branchial cavity, pharynx, oesophagus and/or stomach of four examined clownfish, and large basophilic inclusions within the pharyngeal mucosal epithelium of one fish. Homogenates from pooled external and internal tissues from these outbreaks were inoculated onto striped snakehead (SSN-1) cells for virus isolation and cytopathic effects were observed, resulting in monolayer lysis in the initial inoculation and upon repassage. Transmission electron microscopy of infected SSN-1 cells revealed small round particles (mean diameter=20.0–21.7 nm) within the cytoplasm, consistent with the ultrastructure of a picornavirus. Full-genome sequencing of the purified virus revealed a novel picornavirus most closely related to the bluegill picornavirus and other members of the genus *Limnipivirus*. Additionally, pairwise protein alignments between the clownfish picornavirus (CFPV) and other known members of the genus *Limnipivirus* yielded results in accordance with the current International Committee on Taxonomy of Viruses criteria for members of the same genus. Thus, CFPV represents a proposed new limnipivirus species. Future experimental challenge studies are needed to determine the role of CFPV in disease.

INTRODUCTION

The family *Picornaviridae* currently comprises more than 100 different species, grouped within 47 separate genera [1]. However, many of these species await formal classification, as the number of species and genera has more than doubled over the past few years as a result of increased use of next-generation sequencing (NGS) technologies [1, 2]. Picornaviruses possess non-enveloped round to icosahedral nucleocapsids that are approximately 30 nm in diameter [3, 4]. Within the nucleocapsid lies a single-stranded positive-sense RNA genome, ranging from 6.7 to 10.1 kb in length, which typically contains a single open reading frame (ORF), with the exceptions of canine picodicistrovirus and hedgehog dicipivirus in the genus *Dicipivirus* which contain two [5, 6]. The 3′ end of this genome is polyadenylated, while the 5′ end is covalently linked to a small viral protein,

Received 24 February 2020; Accepted 06 April 2020; Published 18 May 2020
Author affiliations: [1]Department of Infectious Diseases and Immunology, College of Veterinary Medicine, University of Florida, Gainesville, FL, USA; [2]Department of Pathology, University of Texas Medical Branch, Galveston, TX, USA; [3]College of Veterinary Medicine, University of Georgia, Athens, GA, USA; [4]Electron Microscopy Core, Interdisciplinary Center for Biotechnology Research, University of Florida, Gainesville, FL, USA; [5]Experimental Pathology Laboratories, Inc., Sterling, VA, USA; [6]Tropical Aquaculture Laboratory, Program in Fisheries and Aquatic Sciences, School of Forest Resources and Conservation, IFAS, University of Florida, Ruskin, FL, USA.
***Correspondence:** Thomas B. Waltzek, tbwaltzek@ufl.edu
Keywords: clownfish; cell culture; molecular diagnostics; emerging disease; NGS; ornamental aquaculture; picornavirus; PCR; viral discovery.
Abbreviations: BF-2, bluegill fry; CFPV, clownfish picornavirus; EK-1, eel embryonic kidney; EPC, *Epithelioma papulosum cyprini*; FHM, fathead minnow; GF, grunt fin; IACUC, Institutional Animal Care & Use Committee; ICTV, International Committee on Taxonomy of Viruses; RT-PCR, Reverse transcription polymerase chain reaction; SSN-1, striped snakehead; TAL, Tropical Aquaculture Laboratory; TEM, transmission electron microscopy; UTR, untranslated region; WAVDL, Wildlife & Aquatic Veterinary Disease Laboratory.
†Present address: Whitney Laboratory for Marine Bioscience, St Augustine, FL, USA.
GenBank accession numbers MT080321–MT080322.
One supplementary figure and two supplementary tables are available with the online version of this article.

VPg. The 5′ and 3′ ends of the genome have untranslated regions (UTRs), both of which include functionally important secondary structures, such as the internal ribosome entry site within the 5′ UTR, essential for ribosome binding and cap-independent translation. The typical picornavirus genome encodes a single polyprotein that is divided into three regions, P1, P2, and P3. The P1 region contains smaller structural proteins, 1A, 1B, 1C, and 1D, which encode four proteins (VP1–4) responsible for capsid formation and initiation of the virus into host cells through receptor binding. An N-terminus leader protein (L) is also present in some picornavirus genera (e.g. *Aphthovirus* and *Kobuvirus*), preceding the P1 region. The P2 and P3 proteins encode non-structural proteins necessary for viral replication, 2A, 2B, and $2C^{ATPase}$ and 3A, $3B^{VPg}$, $3C^{pro}$, and $3D^{pol}$, respectively. 2A and 2B interfere with host cell functions, while $2C^{ATPase}$ is associated with vesicle formation. The 3A protein is involved with membrane protein presentation and cellular protein transport inhibition, while $3B^{VPg}$, a genome-linked protein, acts as a primer for RNA synthesis during viral replication. The $3C^{pro}$ protein is a protease responsible for the cleavage of the P1 precursor protein, and the $3D^{pol}$ protein is an RNA-dependent RNA polymerase required for viral replication [1, 3, 4, 7]. However, these functions may vary among different picornaviruses [8].

A diversity of picornaviruses have been known to infect a wide variety of animals, although confirmed reports in fish have been limited until recently. Over the last 30 years, fish picorna-like viruses have been isolated in cell cultures and/or visualized by electron microscopy in infected cultures or tissues without sequence confirmation. For example, picorna-like viruses were reported in rainbow and European smelt *Osmerus mordax* and *Osmerus eperlanus* [9, 10], Atlantic salmon *Salmo salar* and other salmonids [11–13], barramundi *Lates calcarifer* [14, 15], turbot *Scophthalmus maximus* [16], sea bass *Dicentrarchus labrax* [17], redspotted grouper *Epinephelis akaara* [18], sandbar shiners *Notropis scepticus* [19], rainbowfish *Melanotaenia lacustris* [20], and common carp *Cyprinus carpio* [21]. However, many of these picorna-like viruses were later genetically characterized as hepeviruses [22] or betanodaviruses (reviewed in [23, 24]).

More recently, four fish viruses were isolated and confirmed by genome sequencing to be picornaviruses. These picornaviruses were isolated from the bluegill *Lepomis macrochirus* [25], common carp [26], fathead minnow *Pimephales promelas* [27], and European eel *Anguilla anguilla* [28]. The bluegill, common carp, and fathead minnow picornaviruses belong to the genus *Limnipivirus*, while the eel picornavirus belongs to the genus *Potamipivirus* [1, 2]. More recently, the genome of a novel potamipivirus was discovered from intestinal tissue samples derived from apparently healthy threespine stickleback *Gasterosteus aculeatus* [29]. Similarly, the genome of a picornavirus derived from the gut tissues of asymptomatic zebrafish *Danio rerio* was determined and found to be divergent enough to constitute the type species of a newly proposed genus, Cyprivirus [30].

In 2018, two studies employing metagenomic approaches resulted in the discovery of 29 new fish picornaviruses, a great leap forward from the handful of previously recognized fish picornavirus species [31, 32]. The sequences of these 29 unclassified fish picornaviruses were determined from specimens that included both wild freshwater and marine species with representatives from lobe-finned (Sarcopterygii), ray-finned (Actinopterygii), and cartilaginous (Chondrichthyes) fishes. In addition to these new fish picornaviruses, another picornavirus was discovered within this timeframe in aquacultured clownfish.

Clownfish are members of the Pomacentridae, a large family containing over 300 species [33, 34]. Members of the family can be found in marine habitats, although a few brackish water species can occasionally be found in fresh water. Pomacentrids primarily inhabit tropical latitudes, with the vast majority residing in the Indo-west and central Pacific regions. Within the family Pomacentridae are four subfamilies, one of which is the Amphiprioninae. This subfamily comprises the *Amphiprion* and *Premnas* genera, and associated species are known informally as clownfish, or anemonefish – so called for their symbiotic relationship with sea anemones [33].

Clownfish are among the most popular marine fishes traded in the international ornamental fish industry, and among them *Amphiprion ocellaris* and *Amphiprion percula* are particularly favoured, along with the maroon clownfish *Premnas biaculeatus* [35]. An estimated 90% of all traded clownfish species are now raised in captivity [36]. In the USA alone, ornamental fish aquaculture is a multimillion-dollar industry [37], while the value of the global marine ornamental trade exceeds USD $300 million per year. It is estimated that two million people participate in this trade worldwide each year, either recreationally or professionally [38, 39].

Over the past decade, a number of aquaculture facilities have experienced large-scale mortality events of unknown aetiology in cultured *A. ocellaris*. In addition to the loss of fish, these disease episodes have caused significant economic losses to these producers [40]. In this investigation, we describe the characterization of a novel picornavirus isolated from moribund *A. ocellaris*, provisionally named the clownfish picornavirus (CFPV). This was achieved through the use of cell culture, histopathology, transmission electron microscopy (TEM), reverse-transcription polymerase chain reaction (RT-PCR), NGS, and phylogenetic analyses.

METHODS

Case histories, parasitology, and histopathology

In 2015, an aquaculture facility experienced chronic morbidity and mortality in juvenile clownfish (*A. ocellaris*) reared in a recirculating system. Diseased fish exhibited a range of non-specific clinical signs, including lethargy, altered body coloration, reduced body condition, tachypnea, and holding an abnormal position in the water column. The water quality of the recirculating system was assessed on-site using a Model FF-3 Saltwater Aquaculture Test kit (Hach Co.) and

recorded as follows: total ammonia: 0 p.p.m.; nitrite: 0 p.p.m.; total alkalinity: 205 p.p.m.; dissolved oxygen: 6.9 p.p.m. (YSI 550A dissolved oxygen meter); salinity: 27 p.p.t. (Vital Sine Salinity Refractomer); pH: 7.87 (Pinpoint pH meter PH370); and water temperature: 26.7 °C.

Ten juvenile clownfish from affected tanks were shipped overnight to the University of Florida Wildlife and Aquatic Veterinary Disease Laboratory (WAVDL) in Gainesville, FL, USA for virological examination, and 20 were shipped to the University of Florida Tropical Aquaculture Laboratory (TAL) in Ruskin, FL, USA for parasitological, bacteriological, and histopathological examination. No healthy fish were submitted for diagnostic evaluation. The weight of the fish ranged from 0.48 to 1.84 g and their total lengths ranged from 2.6 to 4.6 cm. Of the shipped fish, 10 arrived alive at WAVDL and were processed for virus isolation as described below; 13 fish arrived alive at TAL with 8 fish processed for parasitology and bacteriology and 5 fish processed for histopathology.

In 2018, the same aquaculture facility experienced a similar chronic morbidity and mortality event to that described above. The water quality was recorded as follows: total ammonia: 0 p.p.m.; nitrite: 0.23 p.p.m.; total alkalinity: 304.3 p.p.m.; dissolved oxygen: 5.7 p.p.m.; salinity: 22 p.p.t.; pH: 7.86; and water temperature: 30 °C. Eight juvenile clownfish from affected tanks were shipped overnight to WAVDL for virological examination, and an equal number were shipped to TAL for parasitological, bacteriological, and histopathological examination. No healthy fish were submitted for diagnostic evaluation. The weight of the juvenile *A. ocellaris* ranged from 0.7 to 1.8 g and their total lengths ranged from 3.7 to 4.6 cm. Of the eight shipped fish, eight arrived alive at WAVDL and were processed for virus isolation as described below. Of the eight fish shipped to TAL, seven fish arrived alive, with four fish processed for parasitology and bacteriology and three fish processed for histopathology.

For both the 2015 and 2018 cases, parasite burdens were assessed at TAL by examining fin, skin, and gill biopsies. Wet mounts of each tissue biopsy were examined by light microscopy at 40×, 100×, and 200× magnification within 5 min of collection. Immediately following biopsy collection, clownfish were euthanized in 500 mg l^{-1} tricaine methanesulfonate (MS-222, Syndel USA, Tricaine-S®) buffered with an equal concentration of sodium bicarbonate. After euthanasia, bacterial cultures were obtained using sterilized metal loops to aseptically sample brain and posterior kidney for inoculation onto plates of tryptic soy agar (TSA) with 5% sheep blood. Culture plates were incubated at 28 °C for 48 h and were observed daily for the presence/absence of bacterial growth. Following bacteriology, necropsies were conducted, and wet mounts of liver, spleen, anterior kidney, posterior kidney, stomach, and intestine were examined by light microscopy at 40×, 100×, and 200× magnification.

Small ventral body wall incisions were made into the coelomic cavities of five clownfish from the 2015 case and three clownfish from the 2018 case to facilitate fixative penetration, and the fish were placed whole into 10% neutral buffered formalin for 48 h. The fixed fish were cut into multiple transverse slabs through the head and trunk regions and processed by routine histological procedures that included infiltration of the tissues with paraffin, paraffin embedding, microtome sectioning at ~5 µm thickness, and haematoxylin and eosin (H&E) staining. Slides were examined by brightfield microscopy for histopathological changes at 40×, 100×, 200×, and 400× magnification.

Virus isolation

For both the 2015 and 2018 cases, virus isolation was attempted at WAVDL using three cell lines: *Epithelioma papulosum cyprini* (EPC), grunt fin (GF) and striped snakehead (SSN-1). Cell lines were maintained in L-15 media (Leibovitz; Gibco, USA) containing 10% foetal bovine serum (FBS; Gibco, USA), and 1× antibiotic/antimycotic (AA; Gibco, USA), resulting in a final concentration of 100 IP penicillin ml^{-1}, 100 µg streptomycin ml^{-1} and 0.25 µg amphotericin B ml^{-1}. EPC and GF cells were incubated at 21 °C, and SSN-1 cells were incubated at 25 °C.

The submitted clownfish were euthanized using buffered MS-222 at a concentration of 500 mg l^{-1} and divided into pools containing four fish each. Internal (kidney, spleen, and heart) and external (gill and skin) tissue samples were taken from each fish in each of the pools and kept separate. Each of the tissue pools was diluted 1:25 in L-15 media and then homogenized at high speed with a stomacher (Seward stomacher 80, Biomaster Lab system) for 30 s. Two hundred microlitres of each homogenate was pipetted into microcentrifuge tubes and placed on ice for RNA extraction (see below), while the rest of the homogenates were moved to 15 ml conical tubes and used to inoculate cells for virus isolation. The internal and external clownfish tissue homogenates were then centrifuged at 3000 ***g*** for 10 min at 4 °C to pellet cellular debris. The clarified supernatant from each sample was then pipetted into new 15 ml conical tubes, and an equal volume of L-15 media containing 2X AA was added to each tube to make a final dilution of 1:50 and a final concentration of 500 IP penicillin ml^{-1}, 500 µg streptomycin ml^{-1} and 12.5 µg amphotericin B ml^{-1}. The tubes of supernatant were then incubated at 4 °C overnight.

The following day, the supernatant was clarified once again, and 200 µl of each clarified tissue homogenate was inoculated onto triplicate wells of confluent monolayers of EPC, GF, or SSN-1 cells grown within 24-well plates. The plates were rocked every 15 min for 1 h at 21 °C for EPC and GF cells and 25 °C for SSN-1 cells. After this time, the supernatant was removed from each of the infected wells and fresh L-15 media with 2% FBS and 1× AA was added. The EPC and GF plates were then moved to an incubator set at 21 °C, while the SSN-1 plate was incubated at 25 °C. Triplicate negative control wells were inoculated with L-15 supplemented with 2% FBS and 1× AA. All cell lines were monitored daily for the development of cytopathic effects (CPE). Upon the appearance of extensive CPE, the supernatant was clarified and passaged onto recently split cells to

rule out toxicity and confirm that the effects were the result of a passageable agent. Wells that did not display CPE were left for 14 days, after which time the clarified supernatant was passaged onto fresh cells and observed for an additional 14 days before the samples were considered negative. Clarified supernatant from cultures displaying CPE in both the first and second passage were frozen in liquid nitrogen for downstream TEM and genomic sequencing.

TEM

Seventy-five cm^2 flasks of SSN-1 cells displaying CPE were fixed in 15 ml of modified Karnovsky's fixative for 1 h at room temperature, and then washed in cacodylate buffer, scraped and pelleted at 3000 ***g*** for 10 min at 4 °C. The pellet was resuspended in phosphate-buffered saline (PBS) and prepared for TEM as previously described [41] at the University of Florida's Electron Microscopy Core at the Interdisciplinary Center for Biotechnology Research in 2015 and the University of Texas Medical Branch Department of Pathology Electron Microscopy Laboratory (UTMB-EML) in 2018. Photomicrographs were taken of both isolates to examine and measure virion size and structure. The mean capsid diameter for both cases was determined from 60 virus particles using ImageJ2 software [42].

Genomic characterization and phylogenetic analysis

For both CFPV-2015 and CFPV-2018 (the 2015 and 2018 CFPV isolates, respectively), second passage cell lysate from infected flasks of SSN-1 cells was centrifuged at 3000 ***g*** for 10 min at 4 °C in a Beckman–Coulter Allegra X-14R centrifuge to spin down cellular debris. The clarified supernatant was then collected and recentrifuged in a Beckman JA-14 fixed angle rotor at 100000 ***g*** for 90 min at 4 °C to pellet the virus. The supernatant was pipetted off and replaced with resuspension buffer (10 mM Tris-HCl, pH 7.6, 10 mM KCl, 1.5 mM $MgCl_2$) to resuspend the pelleted virus. Baseline-Zero DNase (Lucigen, Middleton, WI, USA) was added to digest extraneous DNA into mononucleotides. The viral RNA (vRNA) was then purified using a RNeasy Mini kit (Qiagen). The purified vRNA served as a template to generate a cDNA library using a NEBNext Ultra RNA Library Prep kit (New England Biolabs, Inc.), which was then sequenced on an Illumina MiSeq sequencer using a 600-cycle v3 MiSeq Reagent kit.

Paired-end sequence reads were then trimmed and *de novo* assembled using CLC Genomics Workbench v11.0 for both CFPV-2015 and CFPV-2018. A BLASTX analysis was used to screen the resulting contigs against a proprietary viral database, built in CLC Genomics Workbench v11.0 from virus protein sequences retrieved from the UniProt Knowledgebase (https://www.uniprot.org/uniprot/). For CFPV-2015, the 5′ end of the genome was determined by using a 5′ Rapid Amplification for cDNA End (RACE) PCR kit (Roche Diagnostics, Mannheim, Germany) and Sanger sequencing. This was not performed on CFPV-2018. The cleavage sites of the CFPV-2015 and CFPV-2018 polyproteins were predicted by sequence alignment comparisons to the polyproteins of other fish picornaviruses within the genus *Limnipivirus* (Table S1, available in the online version of this article) using Geneious R10 [43]. The same approach was implemented in order to predict the polyprotein cleavage sites of three other closely related fish picornaviruses (i.e. Wenling bighead beaked sandfish picornavirus, Guangdong spotted longbarbel catfish picornavirus, and West African lungfish picornavirus) that had not previously been annotated [32].

For phylogenetic analysis, the amino acid (aa) sequences of the $3D^{pol}$ of both the CFPV-2015 and CFPV-2018 isolates were aligned with those of 66 other picornavirus sequences (Table S1) using the Multiple Alignment using Fast Fourier Transform (MAFFT) 7.0 server (https://mafft.cbrc.jp/alignment/software/) with default parameters. A maximum-likelihood tree was generated using 1000 bootstrap replicates in IQ-TREE [44] with default parameters. Pairwise genetic comparisons of the aa sequences of the P1, 2C, 3C, and 3D regions of the CFPV-2015 polyprotein were compared to those of six other closely related fish picornaviruses (Table S1) using the Sequence Demarcation Tool v1.2 [45], with the MAFFT alignment option implemented. Additionally, the full polyproteins of these six fish picornaviruses were aligned and compared with the full polyprotein of CFPV-2015 using Geneious R10.

RNA extraction and development of a CFPV RT-PCR assay

Frozen internal and external tissue homogenates generated in the 2015 and 2018 cases for virus isolation (described above) were subjected to RNA extraction using a RNeasy Mini kit following the manufacturer's instructions (Qiagen). One-step conventional RT-PCR was performed on the extracted RNA samples using a Qiagen OneStep RT-PCR kit and primers targeting the RNA-dependent RNA polymerase ($3D^{pol}$) region of the CFPV-2015 polyprotein (Table 1). These primers, CFPV-F (5′-^{6130}CAGAGAAGAGCACACCCTGG^{6149}-3′) and CFPV-R (5′-^{6385}GCTGGTGCTTTGGTCAACTG^{6366}-3′), were used as follows: after the initial reverse transcription step at 50 °C for 30 min and the denaturation step at 95 °C for 30 min, 40 amplification cycles of 94 °C for 30 s (denaturation), 58 °C for 30 s (annealing), and 72 °C for 30 s (elongation) were

Table 1. CFPV conventional RT-PCR primer set. Primers designed against the CFPV-2015 RNA-dependent RNA polymerase ($3D^{pol}$) gene for use in the conventional RT-PCR diagnostic assay. The CFPV-2015 $3D^{pol}$ gene occurs at nucleotide positions 6047–7513 within the genome, and the amplicon from this primer set occurs at positions 6130–6385

Primer name	Primer sequence	T_m (°C)	Amplicon size including primers (nt)
CFPV-F	CAGAGAAGAGCACACCCTGG	64.5	256
CFPV-R	GCTGGTGCTTTGGTCAACTG	62.4	

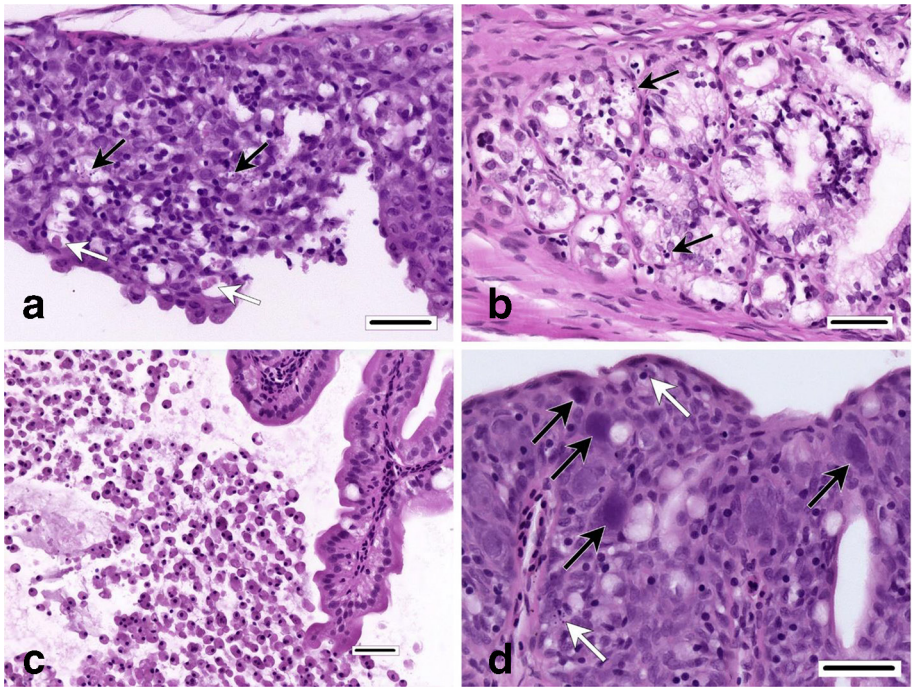

Fig. 1. Histological sections of respiratory and alimentary tracts of a clownfish sampled from a CFPV-positive population. (a) The branchial cavity mucosa appears disrupted and vacuolated, and necrosis is evidenced by the presence of karyorrhectic nuclear debris (black arrows) and phagocytized fragments of cytoplasmic material (white arrows). (b) Necrotic cellular debris (arrows) can be seen frequently in the glandular stomach mucosa. (c) Abundant exfoliated cells in the proximal intestine lumen of a fish in which gastric gland necrosis was observed. (d) Large basophilic inclusions (black arrows) in epithelial cells of the pharyngeal mucosa, accompanied by occasional necrotic cells (white arrows). H&E stain. All images, bar=25 µm.

carried out, followed by a final elongation step at 72 °C for 5 min. Reaction volumes were 30 µl and consisted of 8.4 µl of molecular grade water, 6 µl of 5× RT-PCR buffer, 6 µl of 5× Q solution, 1.2 µl of 10 mM dNTPs, 1.2 µl each of 20 µm forward and reverse primers, 1.2 µl of RT-PCR enzyme mix, and 4.8 µl of RNA template. Following 1% agarose gel electrophoresis, bands of the expected size (256 bp amplicon including primers) were purified using a Qiagen QIAquick Gel Extraction kit and submitted to Eurofins Genomics (USA) to be confirmed by Sanger sequencing.

Testing archived clownfish tissue samples by RT-PCR

WAVDL received clownfish specimens from two different facilities experiencing similar disease episodes in their cultured *A. ocellaris* in the years 2011, 2012, 2014, 2015, 2017, and 2018. The CFPV conventional RT-PCR assay described above was used to screen archived RNA extracts generated from the gill tissue of a representative *A. ocellaris* from each disease episode from 2011 to 2018. A gill tissue RNA extract was also tested in 2019 from an *A. ocellaris* as part of a healthy-appearing aquacultured stock to serve as a negative control.

RESULTS

Parasitology, bacteriology, and histopathology

In both the 2015 and 2018 cases, bacteriological and parasitological examinations did not yield significant bacterial or parasitic burdens. However, histopathological lesions potentially consistent with a viral aetiology were evident in four examined fish from the 2015 outbreak (Fig. 1). Such findings included minimal to moderate individual cell necrosis and mononuclear cell inflammation in mucosal epithelia of the branchial cavity, pharynx, oesophagus and/or stomach. Mucosal epithelial necrosis was characterized by cytoplasmic and nuclear fragmentation (karyorrhexis), accompanied by occasional cell loss. In one fish, necrosis of gastric glands was associated with accumulations of exfoliated cells in the proximal intestine. In another of the four clownfish, several round to oval basophilic inclusions (10–15 µm diameter) were evident within the mildly hyperplastic pharyngeal mucosal epithelium, in which low to moderate numbers of lymphocytes and infrequent necrotic cells were also present. Due to their large size, the precise subcellular location of these inclusions (i.e. nuclear vs cytoplasmic) was difficult to determine in the H&E sections. A histopathological workup in the 2018 case did not reveal significant microscopic lesions.

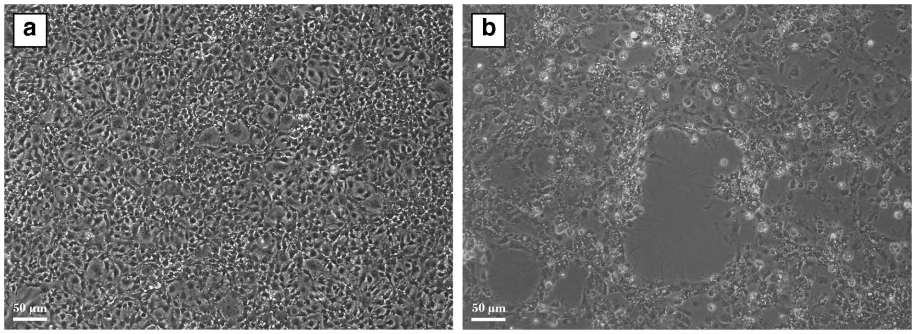

Fig. 2. *In vitro* growth characteristics of the CFPV-2015 isolate in striped snakehead (SSN-1) cells. (a) Uninfected SSN-1 cells, day 8 post-inoculation. (b) Infected SSN-1 cells, day 8 post-inoculation.

Virus isolation

CPE were observed on the SSN-1 cell line within 3 days post-inoculation of the 2015 and 2018 pooled external and internal tissue homogenates. Cellular changes included enlargement and refractility of cells, and the development of round plaques that eventually coalesced to result in complete destruction of the cellular monolayer by day six (Fig. 2). The clarified SSN-1 supernatants in both years were passaged onto fresh SSN-1 cells and again resulted in complete destruction of the monolayers. No CPE were observed in the EPC or GF cell lines over the course of the incubation period (14 days) or in the subsequent passage onto confluent monolayers of EPC and GF cells in either year.

TEM

Analysis of the infected SSN-1 cells from the 2015 case using TEM revealed non-enveloped spherical virus particles within the cell cytoplasm (Fig. 3). The particles were observed individually and as part of paracrystalline arrays. Similar ultrastructural features were also noted in the 2018 case. The mean diameter and standard deviation (SD) of the virus particles from the 2015 and 2018 cases were 20.0 nm (n=60, SD=1.05 nm) and 21.7 nm (n=60, SD=2.6 nm), respectively. We attributed the significant difference (comparison by t-test, P<0.05) in particle diameter between the years to have resulted from differences in sample processing and photomicroscopy between the electron microscopy facilities.

Genomic characterization and phylogenetic analysis

The complete CFPV genome sequence from the 2015 isolate was determined to be 8166 bp and predicted to have a 3–4–4 genome layout: 5′UTR-P1(1AB-1C-1D)-P2(2A1-2A2-2B-2C)-P3(3A-3B-3C-3D)-3′UTR (Fig. 4). The 5′ and 3′ UTRs of CFPV-2015 were determined to be 571 and 423 bp, respectively. BLASTN analysis of the 5′ UTR of CFPV-2015 showed no homology to other limnipiviruses. A single ORF encoding a putative multi-functional polyprotein of 2314

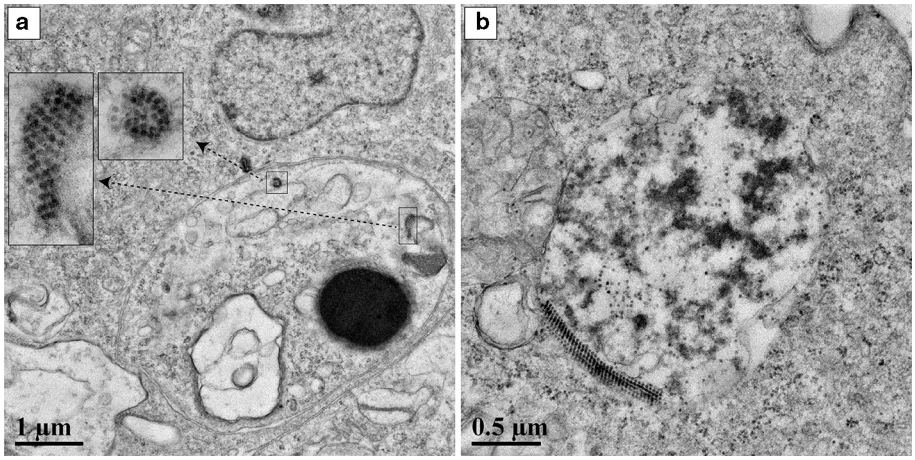

Fig. 3. Ultrastructural features of the CFPV-2015 isolate in striped snakehead (SSN-1) cells. (a) Electron micrograph of CFPV-2015 displaying non-enveloped round particles with a mean diameter of 20 nm within the cytoplasm of an infected SSN-1 cell. Arrows indicate higher magnification of the virus particles. (b) Electron micrograph of CFPV-2015 particles arranged in a paracrystalline array within the cytoplasm of an infected SSN-1 cell.

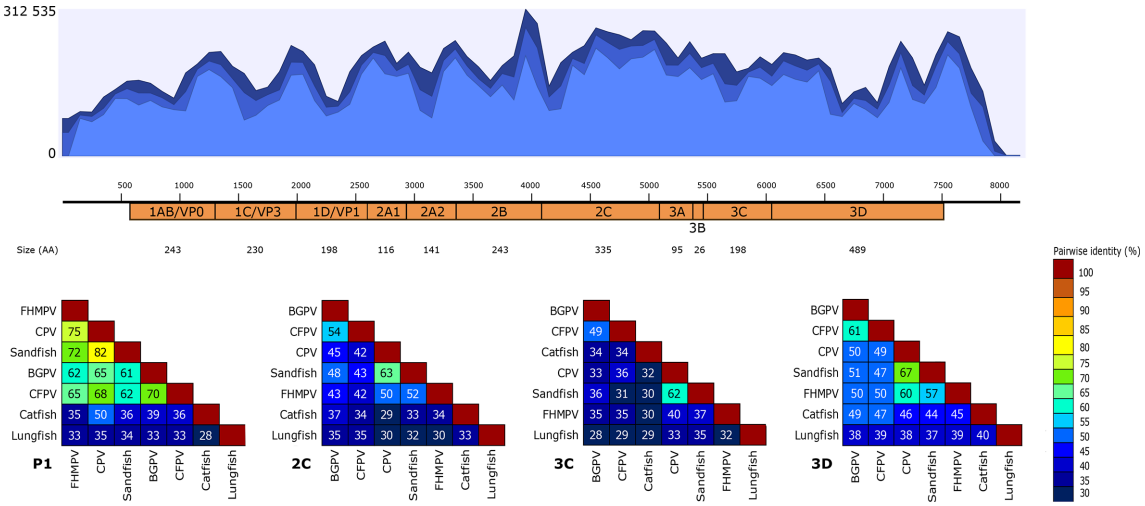

Fig. 4. Annotated CFPV-2015 polyprotein showing predicted cleavage sites and functional domains (orange), alongside a map of the CFPV-2015 genome showing read coverage from the MiSeq data. Different shades of blue from top to bottom show the maximum, average and minimum coverage values, as calculated using a window size of 1 bp. Sequence identity matrices are shown below for P1, 2C, 3C, and 3D regions of CFPV-2015 compared with those of the bluegill picornavirus (BGPV), fathead minnow picornavirus (FHMPV), carp picornavirus (CPV), sandfish picornavirus, catfish picornavirus, and lungfish picornavirus.

aa was identified in CFPV-2015 and CFPV-2018 (Table S2). The P1 region of both isolates was determined to be 671 aa long and encoded structural proteins (i.e. capsid proteins). Similarly, the P2 and P3 regions were 835 and 808 aa long, respectively, and encoded non-structural proteins. Like limnipiviruses, the CFPV-2015 and CFPV-2018 isolates did not possess a leader peptide and the 2C region included a Walker A GxxGxGKS (GKPGQGKT; aa 1308–1315) motif. In both isolates, the putative 3C protease region included a GxCGx$_{10\text{-}15}$GxH (GYCGSLILQKQYGTWKIVAMH; aa 1784–1804) motif. The 3D polymerase of the CFPV-2015 and CFPV-2018 isolates included the following conserved motifs: KDE (aa 1994–1996), DxxxxD (DYSKFD; aa 2070–2075), PSG (aa 2126–2128), YGDD (aa 2171–2174), and FLKR (aa 2219–2222).

The maximum-likelihood analysis based on the 3D^{pol} aa sequence alignment among different picornavirus genera yielded a well-supported and highly resolved tree, with bootstrap replicate values of 100% for most nodes (Fig. 5). CFPV-2015 and CFPV-2018 were supported as each other's closest relative and together they branched as the sister species to the bluegill picornavirus (BGPV), with bootstrap support of 100%. The CFPV and BGPV clade was supported as the sister group to a well-supported clade composed of the other two limnipiviruses (i.e. fathead minnow picornavirus and the carp picornavirus), as well as an unclassified Wenling bighead beaked sandfish picornavirus. Two other unclassified picornaviruses, the spotted longbarbel catfish and the West African lungfish picornaviruses, formed well-supported basal branches to the aforementioned limnipivirus clades. The P1, 2C, 3C, and 3D regions of CFPV-2015 showed 99, 99.7, 99.5, and 99.5% aa identity to CFPV-2018, respectively. The P1 region of the CFPV-2015 isolate exhibited greatest (70%) aa identity to that of the BGPV, while its 2C, 3C, and 3D displayed 54, 49, and 61 % identity to the BGPV, respectively (Fig. 4). Comparison of the full CFPV-2015 polyprotein to the polyproteins of six other fish picornaviruses revealed similar cleavage products (Fig. S1).

Development of a CFPV RT-PCR assay

The CFPV RT-PCR assay yielded positive results for all of the pooled tissue homogenate samples generated in the 2015 and 2018 cases. Sanger sequencing of the purified PCR products resulted in identical sequences to the corresponding CFPV-2015 and CFPV-2018 sequences generated by the Illumina MiSeq sequencer. The archived samples from diseased *A. ocellaris* in the years 2011–2018 all produced the expected amplicons and yielded sequences with >99% nucleotide identity to the 2015 and 2018 sequences. The gill tissue sample collected from a healthy-appearing aquacultured *A. ocellaris* in 2019 yielded negative results.

DISCUSSION

In this study, we characterized a novel clownfish picornavirus (CFPV) isolated from diseased *A. ocellaris,* the first report of a picornavirus isolated from a maricultured ornamental fish. The growth of CFPV in SSN-1 cells in both the 2015 and 2018 cases facilitated its downstream ultrastructural and genomic characterization. The CFPV virion architecture and development was congruous with typical picornavirus virion morphogenesis, including the observation of small, non-enveloped, round virus particles within the cytoplasm of the infected SSN-1 cells. The size, shape, and location of the CFPV nucleocapsids are consistent with reports of other picornaviruses, including those previously isolated from fish

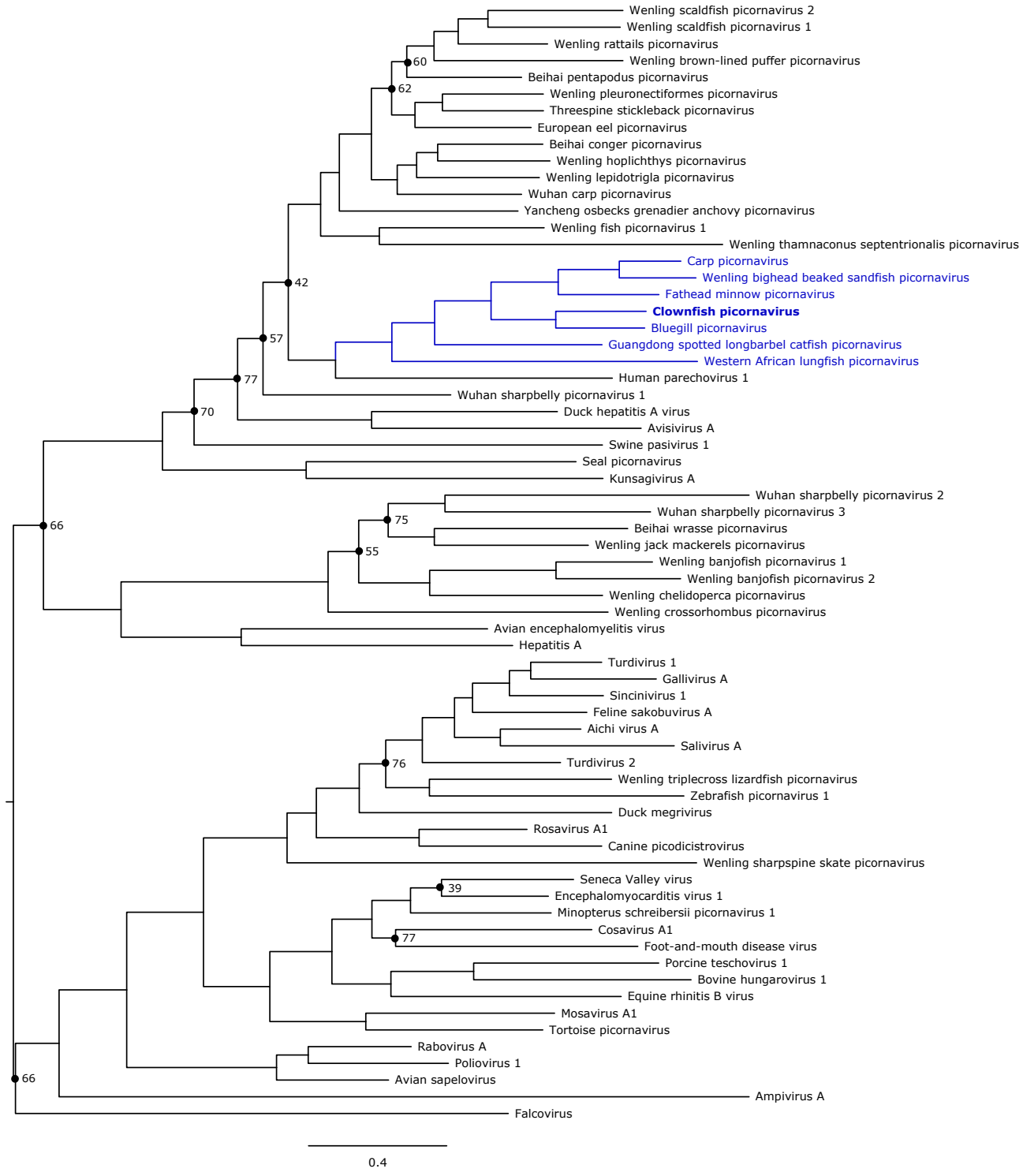

Fig. 5. Maximum-likelihood phylogram based on the amino acid sequence of the complete $3D^{pol}$ gene of 68 picornaviruses. Taxa shown in blue are fish picornaviruses forming a clade with the two clownfish picornavirus isolates, while those shown in black represent the type species from all other known picornavirus genera, as well as all other known fish picornaviruses. All nodes are supported by bootstrap values >80% (with the exception of those with nodes marked with '•'). Inferred substitutions are represented by the lengths of each branch as indicated by the scale bar.

[25–30]. The genomic and phylogenetic analyses strongly supported CFPV as a novel species and closest relative to the BGPV within the fish picornavirus genus *Limnipivirus*. Finally, a specific conventional RT-PCR assay was designed as a rapid screening tool to test *A. ocellaris* tissues for the presence of CFPV. The RT-PCR assay detected CFPV in archived samples from moribund *A. ocellaris* dating back as far as 2011.

The CFPV-2015 genome was determined to be 7939 nucleotides in length before the poly(A) tract, while the genomes of the European eel, bluegill, common carp, fathead minnow, zebrafish, and threespine stickleback picornaviruses are 7632, 7834, 8050, 8298, 8404, and 7496 nucleotides, respectively [25–30]. The CFPV 5′ UTR (571 bp) and 3′ UTR (423 bp) are longer than those of other limnipiviruses (501–712 bp and 38–342 bp, respectively). In addition, the serine (S) in the Walker A GxxGxGKS motif of the 2C helicase is replaced by a threonine (T), as in all limnipiviruses.

Genetic analysis of regions of the CFPV polyprotein revealed that it shares the closest amino acid identity to the BGPV, a limnipivirus. Similarly, the phylogenetic analysis based on the RNA-dependent RNA polymerase ($3D^{pol}$) gene yielded a tree in which CFPV grouped within the genus *Limnipivirus* as the closest relative to the BGPV. The CFPV and BGPV clade was supported as the sister group to the other limnipiviruses, the fathead minnow picornavirus (FHMPV) and the carp picornavirus (CPV). Unclassified fish picornaviruses, the Guangdong spotted longbarbel catfish picornavirus and the West African lungfish picornavirus, formed well-supported branches basal to the currently accepted limnipiviruses. According to the current International Committee on Taxonomy of Viruses (ICTV) guidelines, the criteria used for the picornavirus genus and species demarcations are based on the genetic distances between P1, 2C, 3C, and 3D. Picornaviruses with aa sequence divergence exceeding 66% for P1 and 64% for 2C, 3C, and 3D are considered to be members of different genera [1]. Within the genus *Limnipivirus,* those with aa sequence divergence ranges of 30–43% for P1 and 49–57% for 3C and 3D are considered different species [1]. The observed aa sequence divergences of the CFPV P1, 2C, 3C, and 3D proteins to accepted limnipiviruses (i.e. BGPV, CPV, and FHMPV) ranged from 30–35%, 46–58%, 51–65%, and 39–51%, respectively, supporting its inclusion as a new species in the genus (Fig. 4).

The aa sequence divergences of the Wenling bighead beaked sandfish picornavirus P1, 2C, 3C, and 3D compared to the other known limnipiviruses ranged between 18–39%, 37–52%, 38–64%, and 33–49%, respectively, while those of the Guangdong spotted longbarbel catfish picornavirus ranged from 50–65%, 63–71%, 66–70%, and 51–55%, and those of the West African lungfish picornavirus ranged from 65–67%, 65–70%, 67–72%, and 61–62%. From these genetic distances, we posit that the Wenling bighead beaked sandfish picornavirus should also be included as a new species within the genus *Limnipivirus*, while both the Guangdong spotted longbarbel catfish picornavirus and the West African lungfish picornavirus represent novel species within yet-to-be-defined genera. This work thus provides an important update to the taxonomy (and biology) of fish picornaviruses both within and outside the genus *Limnipivirus*. Consideration of CFPV and the Wenling bighead beaked sandfish picornavirus as new limnipivirus species will require formal proposal to, and ratification by, the ICTV.

To date, most fish picornaviruses have been detected in wild fish, including European eel, fathead and brassy *Hybognathus hankinsoni* minnows, bluegill, threespine stickleback, and 29 other freshwater and marine fishes [25, 27–29, 31, 32]. In contrast, picornaviruses from carp and zebrafish, along with fathead minnows, have been characterized from aquacultured or laboratory-managed stocks [26, 27, 30]. CFPV represents the first picornavirus characterized from an important maricultured ornamental species, the clownfish *A. ocellaris*.

The majority of fish picornaviruses have not been grown in *in vitro* cultures, and thus, the role of many of these viruses (if any) in disease remains to be determined [29–32]. Isolation of fish picornaviruses has typically involved cell lines derived from the same host or a closely related host. For example, the carp and fathead minnow picornaviruses were isolated on cell lines derived from cyprinids (i.e. FHM and EPC), the eel picornavirus was isolated on the eel embryonic kidney (EK-1) cell line, and the bluegill picornavirus was isolated on the bluegill fry (BF-2) cell line. In contrast, CFPV grew on a cell line (SSN-1) derived from a freshwater fish (striped snakehead; *Channa striata*). CFPV did not grow on the EPC cell line or the grunt fin cell line derived from a marine fish (blue-striped grunt; *Haemulon sciurus*). Although the bluegill, carp, clownfish, and eel picornaviruses were isolated from moribund fish [25, 26, 28], the fathead minnow picornavirus was isolated from seemingly healthy fathead and brassy minnows [27].

The role of picornaviruses as disease-causing agents of fish has only recently received significant attention. Picornaviruses isolated from wild European eels and bluegill were capable of inducing disease under controlled laboratory conditions [25, 28], while another picornavirus isolated from aquacultured common carp was not [26]. Experimental challenges were not performed in studies involving picornaviruses characterized from wild fathead minnows [27], threespine stickleback [29], or managed zebrafish [30]. Recent studies employing metagenomics detected numerous picornavirus sequences across a range of fishes, irrespective of their health status [31, 32]. Although the role of CFPV in disease remains undetermined, we confirmed CFPV RNA by RT-PCR in archived clownfish tissue extracts (*A. ocellaris* and *A. percula*) from mass mortality events that had occurred at two USA clownfish production facilities between the years 2011 and 2018, but not from a single fish collected in 2019 from a population of apparently healthy fish.

The role of CFPV as a causative agent of disease was not clearly established in the present study. Interestingly, the microscopic lesions observed in the 2015 case were not observed in the 2018 case. The lack of histopathological

findings in the 2018 fish may be attributed to the sampling of unaffected or mildly affected animals, or fish that had already begun the recovery phase. For certain viral infections, morphological effects may only be evident within a narrow window of time during the natural course of the disease. It is also possible that the branchial and gastrointestinal lesions observed in the 2015 case were not the result of CFPV infection. Future challenge studies are needed to fulfil River's postulates in order to better understand the mode of transmission and relevance of CFPV to the morbidity and mortality events observed at these facilities [46].

The discovery of CFPV may have significant implications for the marine ornamental industry, as clownfish epizootics over the past decade have led to production lapses and significant economic losses for some facilities in the USA [40]. If CFPV is determined to be the cause of these aquaculture epizootics, it will be necessary to develop effective management strategies to mitigate the disease and help prevent over-collection of wild fish from coral reefs. In addition to the financial consequences for clownfish culture facilities, wild collection of clownfish can be an ecologically damaging process, especially in the case of cyanide fishing [47]. Given the potential damage caused by CFPV, as well as the increasing number of picornaviruses that have been isolated from wild fish, it seems important to ascertain whether its significance extends beyond aquaculture. Therefore, future studies should investigate the prevalence and disease potential of CFPV for wild populations of *A. ocellaris*.

Funding information
This work received no specific grant from any funding agency.

Author contributions
E. C. S., conceptualization, investigation, formal analysis, visualization, data curation, writing – original draft preparation, writing – review and editing. K. S., conceptualization, formal analysis, visualization, validation, writing – original draft preparation, writing – review and editing. L. A. H., investigation, writing – review and editing. K. I., investigation, writing – review and editing. P. M. T., investigation. V. L. P., conceptualization, visualization, investigation, resources, writing – review and editing. T. F. F., conceptualization, investigation, writing – review and editing. K. L. K., investigation, writing – review and editing. R. A., investigation, writing – review and editing. J. C. W., conceptualization, investigation, writing – review and editing. D. B. P., investigation, writing – review and editing. R. P. E. Y., conceptualization, investigation, writing – review and editing. T. B. W., conceptualization, project administration, resources, validation, investigation, writing – review and editing, writing – original draft preparation, supervision.

Conflicts of interest
The authors declare that there are no conflicts of interest.

Ethical statement
No experimental licenses were required for this work. All viral isolates were obtained from farmed fish during veterinary investigations.

References

1. Zell R, Delwart E, Gorbalenya AE, Hovi T, King AMQ *et al*. ICTV Virus Taxonomy Profile: *Picornaviridae*. *J Gen Virol* 2017;98:2421–2422.
2. King AMQ, Lefkowitz EJ, Mushegian AR, Adams MJ, Dutilh BE *et al*. Changes to taxonomy and the International Code of virus classification and nomenclature ratified by the International Committee on taxonomy of viruses (2018). *Arch Virol* 2018;163:2601–2631.
3. Racaniello VP. *Picornaviridae*: The viruses and their replication. In: Knipe DM, Howley PM (editors). *Fields Virology*, 6th ed. Philadelphia, PA: Lippincott Williams & Wilkins; 2013. pp. 453–489.
4. Jiang P, Liu Y, Ma H-C, Paul AV, Wimmer E. Picornavirus morphogenesis. *Microbiol Mol Biol Rev* 2014;78:418–437.
5. Woo PCY, Lau SKP, Choi GKY, Huang Y, Teng JLL *et al*. Natural occurrence and characterization of two internal ribosome entry site elements in a novel virus, canine picodicistrovirus, in the picornavirus-like superfamily. *J Virol* 2012;86:2797–2808.
6. Reuter G, Boros Ákos, Földvári G, Szekeres S, Mátics R *et al*. Dicipivirus (family *Picornaviridae*) in wild Northern white-breasted hedgehog (*Erinaceus roumanicus*). *Arch Virol* 2018;163:175–181.
7. Lin J-Y, Chen T-C, Weng K-F, Chang S-C, Chen L-L *et al*. Viral and host proteins involved in picornavirus life cycle. *J Biomed Sci* 2009;16:103.
8. TFF N. Personal observation 2019.
9. Moore AR, LI MF, McMENEMY M. Isolation of a picorna-like virus from smelt, *Osmerus mordax* (Mitchill). *J Fish Dis* 1988;11:179–184.
10. Ahne W, Anders K, Halder M, Yoshimizu M. Isolation of picornavirus-like particles from the European smelt, *Osmerus eperlanus* (L.). *J Fish Dis* 1990;13:167–168.
11. Hedrick RP, McDowell TS, Kent ML, Elston RA. A small RNA virus isolated from Atlantic salmon (*Salmo salar*). *J Appl Ichthyol* 1990;6:173–181.
12. Hedrick RP, Yun S, Wingfield WH. A small RNA virus isolated from salmonid fishes in California, USA. *Can J Fish Aquat Sci* 1991;48:99–104.
13. Eaton WD, Bagshaw J, Hulett J, Evans S. Isolation of a picorna-like virus from steelhead in Washington state. *J Aquat Anim Health* 1992;4:90–96.
14. Glazebrook JS, Heasman MP, BEER SW. Picorna-like viral particles associated with mass mortalities in larval barramundi, *Lates calcarifer* Bloch. *J Fish Dis* 1990;13:245–249.
15. Munday BL, Langdon JS, Hyatt A, Humphrey JD. Mass mortality associated with a viral-induced vacuolating encephalopathy and retinopathy of larval and juvenile barramundi, *Lates calcarifer* Bloch. *Aquaculture* 1992;103:197–211.
16. Bloch B, Gravningen K, Larsen JL. Encephalomyelitis among turbot associated with a picornavirus-like agent. *Dis Aquat Organ* 1991;10:65–70.
17. Breuil G, Bonami JR, Pepin JF, Pichot Y. Viral infection (picorna-like virus) associated with mass mortalities in hatchery-reared sea-bass (*Dicentrarchus labrax*) larvae and juveniles. *Aquaculture* 1991;97:109–116.
18. Mori K-ichiro, Nakai T, Nagahara M, Muroga K, Mekuchi T *et al*. A viral disease in hatchery-reared larvae and juveniles of redspotted grouper. *Fish Pathol* 1991;26:209–210.
19. Iwanowicz LR, Goodwin AE, Heil N. A small RNA virus isolated from apparently healthy wild sandbar shiners, *Notropis scepticus* (Jordan & Gilbert). *J Fish Dis* 2000;23:349–352.
20. Petty BD, Fraser WA. Viruses of PET fish. *Vet Clin North Am Exot Anim Pract* 2005;8:67–84.
21. Reuter G, Pankovics P, Delwart E, Boros Ákos. A novel posavirus-related single-stranded RNA virus from fish (*Cyprinus carpio*). *Arch Virol* 2015;160:565–568.
22. Batts W, Yun S, Hedrick R, Winton J. A novel member of the family Hepeviridae from cutthroat trout (Oncorhynchus clarkii). *Virus Res* 2011;158:116–123.
23. Bovo G, Florio D. Viral diseases of cultured marine fish. In: Eiras JC, Segner H, Wahli T, Kapoor BG (editors). *Fish Diseases*, 1st ed. Science Publishers: Enfield, NH; 2008. pp. 185–238.
24. Walker PJ, Winton JR. Emerging viral diseases of fish and shrimp. *Vet Res* 2010;41:51.
25. Barbknecht M, Sepsenwol S, Leis E, Tuttle-Lau M, Gaikowski M *et al*. Characterization of a new picornavirus isolated from the freshwater fish *Lepomis macrochirus*. *J Gen Virol* 2014;95:601–613.

26. Lange J, Groth M, Fichtner D, Granzow H, Keller B *et al*. Virus isolate from carp: genetic characterization reveals a novel picornavirus with two aphthovirus 2A-like sequences. *J Gen Virol* 2014;95:80–90.
27. Phelps NBD, Mor SK, Armien AG, Batts W, Goodwin AE *et al*. Isolation and molecular characterization of a novel picornavirus from baitfish in the USA. *PLoS One* 2014;9:e87593.
28. Fichtner D, Philipps A, Groth M, Schmidt-Posthaus H, Granzow H *et al*. Characterization of a novel picornavirus isolate from a diseased European eel (*Anguilla anguilla*). *J Virol* 2013;87:10895–10899.
29. Hahn MA, Dheilly NM. Genome characterization, prevalence, and transmission mode of a novel picornavirus associated with the threespine stickleback fish (*Gasterosteus aculeatus*). *J Virol* 2019;93:e02277–18.
30. Altan E, Kubiski SV, Boros Ákos, Reuter G, Sadeghi M *et al*. A highly divergent picornavirus infecting the gut epithelia of zebrafish (*Danio rerio*) in research institutions world-wide. *Zebrafish* 2019;16:291–299.
31. Geoghegan JL, Di Giallonardo F, Cousins K, Shi M, Williamson JE *et al*. Hidden diversity and evolution of viruses in market fish. *Virus Evol* 2018;4:vey031.
32. Shi M, Lin X-D, Chen X, Tian J-H, Chen L-J *et al*. The evolutionary history of vertebrate RNA viruses. *Nature* 2018;556:197–202.
33. Fautin DG, Allen GR. *Field Guide to Anemone Fishes and Their Host Sea Anemones*. Perth: Western Australian Museum; 1992.
34. Sin TM, Teo MM, Ng PKL, Chou LM, Khoo HW. The damselfishes (Pisces: Osteichthyes: Pomacentridae) of Peninsular Malaysia and Singapore: systematics, ecology and conservation. *Hydrobiologia* 1994;285:49–58.
35. Patkaew S, Direkbusarakom S, Tantithakura O. A simple method for cell culture of 'Nemo' ocellaris clownfish (*Amphiprion ocellaris*, Cuvier 1830). *Cell Bio Int Rep* 2014;21:39–45.
36. King TA. Wild caught ornamental fish: a perspective from the UK ornamental aquatic industry on the sustainability of aquatic organisms and livelihoods. *J Fish Biol* 2019;94:925–936.
37. Watson CA, Shireman JV. *Production of Ornamental Aquarium Fish*. University of Florida IFAS Extension; 2002.
38. Wabnitz C, Taylor M, Green E, Razak T. From ocean to aquarium: a global trade in marine ornamental species. UNEP world conservation and monitoring centre (WCMC) 2003.
39. Sirajudheen TK, Shyam SS, Bijukumar A, Bindu A. Problems and prospects of marine ornamental fish trade in Kerala, India. *J Fish Econ & Dev* 2014;15:14–30.
40. Yanong R. Personal observation 2018.
41. Ahasan MS, Subramaniam K, Sayler KA, Loeb JC, Popov VL *et al*. Molecular characterization of a novel reassortment *mammalian orthoreovirus* type 2 isolated from a Florida white-tailed deer fawn. *Virus Res* 2019;270:197642.
42. Schindelin J, Rueden CT, Hiner MC, Eliceiri KW. The ImageJ ecosystem: an open platform for biomedical image analysis. *Mol Reprod Dev* 2015;82:518–529.
43. Kearse M, Moir R, Wilson A, Stones-Havas S, Cheung M *et al*. Geneious basic: an integrated and extendable desktop software platform for the organization and analysis of sequence data. *Bioinformatics* 2012;28:1647–1649.
44. Nguyen L-T, Schmidt HA, von Haeseler A, Minh BQ. IQ-TREE: a fast and effective stochastic algorithm for estimating maximum-likelihood phylogenies. *Mol Biol Evol* 2015;32:268–274.
45. Muhire BM, Varsani A, Martin DP. SDT: a virus classification tool based on pairwise sequence alignment and identity calculation. *PLoS One* 2014;9:e108277.
46. Rivers TM. Viruses and Koch's postulates. *J Bacteriol* 1937;33:1–12.
47. Dee LE, Horii SS, Thornhill DJ. Conservation and management of ornamental coral reef wildlife: successes, shortcomings, and future directions. *Biol Conserv* 2014;169:225–237.